LM Flight Simulation in the Space Environment

M. N. Tawil* and A. A. Ferrara†
Grumman Aerospace Corp., Bethpage, N. Y.

This paper deals with the ground test verification of the Lunar Module (LM) readiness for flight in the thermal, vacuum environment of space and the lunar surface. Complete-vehicle, worst-case mission simulation tests, certifying those missions representing reasonable flight schedule confidence levels, are presented as the logical wrap-up to subsystem evaluation. The configuration and ground test modifications imposed on a typical flight LM to enable mission simulation testing are described. Thermal simulation of the external environment through the use of conformal skin heaters, as well as test simulation difficulties, are treated in detail. The program's role in the verification of the thermal analytical techniques used for flight and design evaluation is described. A comparison of flight to test data for the Apollo 10, 11, and 12 missions is presented. In general, results show that the analytical models, as modified by test results, can predict flight response to within 5°F.

Introduction

Vehicle Configuration

THE Apollo Lunar Module (LM) is the first true manned spacecraft to be flown from Earth. It is designed to operate solely in the rather severe environment of space, and has no provisions for a return to Earth.[1] It comprises an ascent stage (A/S, Fig. 1) and descent stage (D/S, Fig. 2). The A/S houses the crew, most of the electronics, control and life support equipment.

The A/S consists of three major segments: the main cabin, the midbody, and the aft equipment bay (AEB). The cabin contains the control panels and displays, and forms the main section of the crew compartment. The guidance system is mounted atop the cabin pressure shell. The aft portion of the cabin forms the core of the midbody, with the main propulsion and reaction control system (RCS) tanks mounted on both sides. The A/S engine is installed below the midbody and protrudes into the cabin space. Atop the midbody is the docking tunnel with a water tank on either side. The AEB contains the A/S propulsion system (APS) helium tanks and most of the electronic equipment that is actively cooled by the Environmental Control System (ECS) glycol loop. The RCS clusters and antennas are mounted at various points on the A/S.

The D/S is the carrier which enables lunar landing and provides consumables for the lunar stay, as well as storage for various experiment packages used on the moon. Its basic cruciform structure is enclosed by side, top, and bottom panels. Propellant tanks for the D/S Propulsion System (DPS) are located in four rectangular compartments. They contain water and helium tanks, batteries, and scientific equipment to be utilized after landing. The gimbaled D/S engine is located in the center bay. External hardware includes the landing radar and the landing gear with its associated deployment mechanisms.

Both stages depend upon multilayer insulation for thermal isolation of the interior hardware from the external environment.[2]

Mission Description

The Apollo LM missions may be separated into discrete phases as follows:

1) Earth orbit—For the lunar missions (LM-4 and subsequent), this phase is not thermally significant due to its relative brevity (~2 hr) and the fact that the LM is shielded by the Spacecraft-LM Adapter (SLA) from the space environment.

2) Translunar flight—This period can last from 60 to 100 hr. During this time, the crew remains in the Command Module (CM) and the LM is essentially dormant. The mated vehicles alternately spin or "barbecue" about the cylindrical axis at 1 rph and hold fixed attitudes for star-sighting and mid-course maneuvers; there is no thermal constraint on the hold orientation.

3) Lunar orbit—During this phase (~25 hr) two of the astronauts enter and activate the LM, separate from the CM, and prepare for the lunar descent. On the Apollo 10 (LM-4) mission typical lunar lander operations were performed with the exception of a powered descent burn to the lunar surface.

4) Lunar descent and landing—The DPS is used to deorbit the spacecraft and control the descent prior to lunar touchdown.

5) Lunar stay—The LM remains on the lunar surface for up to 35 hr; it is always in the sun with its systems active. Thermal soakback from the DPS firing is a major heating effect on the D/S. Astronaut traffic into and out of the LM triggers significant changes in the vehicle thermal status. Thermal control during active periods is primarily governed by the ECS.

6) Lunar liftoff, rendezvous, and docking—This phase can be from 3 to 12 hr in length and begins when the A/S separates from the D/S. Using the latter as a launch platform, the APS lifts the A/S into orbit and eventual rendezvous with the CM. This is the peak heating phase for the A/S due to engine soakback. At the end of this phase the A/S is jettisoned.

To date, two vehicles (Apollo's 11 and 12) have successfully flown the basic flight timeline outlined.

Mission Simulation Testing

The LTA-8 test program was designed to demonstrate the ability of the LM to perform its planned mission under simulated thermal-vacuum conditions. In addition, the program was to verify the ability of the analytical thermal networks to accurately predict vehicle thermal response. To accomplish this goal, a production-type LM would be operated in accordance with an actual flight mission timeline

Presented as Paper 69-999 at the AIAA/ASTM/IES 4th Space Simulation Conference, Los Angeles, Calif., September 8–10, 1969; submitted September 29, 1969; revision received February 5, 1970. This work was performed for the NASA Manned Spacecraft Center, under Contract NAS-9-1100.

* System Manager, Space Station Thermodynamics.
† Unit Leader, LM Vehicle Thermal Balance. Member AIAA.

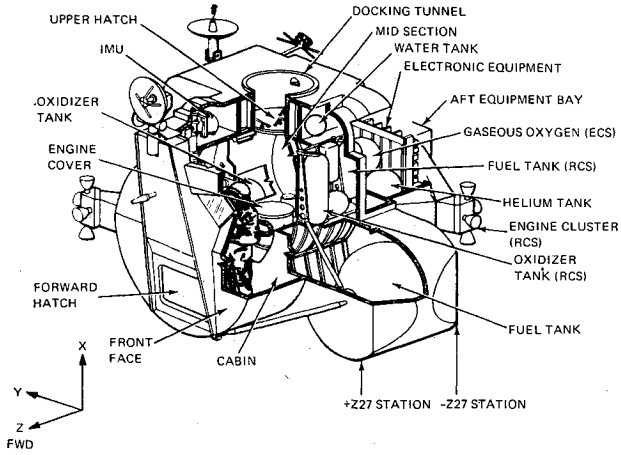

Fig. 1 Ascent stage (A/S) general arrangement.

while under test. The external environment would simulate the real flight while all of the internal LM systems were being exercised in the proper mission sequence. The firing of various rocket engines, astronaut mannings, equipment operations, etc., were to be performed in an operational sequence synchronized to follow the actual planned flight operations timeline.

Simulating a single nominal mission was judged to be insufficient to prove performance. By referring to the contractual Thermal Design Mission,[3] it was noted that a large matrix of mission timelines, equipment duty cycles, etc., was possible. However, all such cases could be bound by two worst-case missions which would drive the vehicle toward its high- and low-temperature extremes, thus exercising the many subtle system interactions which might be lost in analyses or in a disjointed series of piecemeal tests. To define acceptable performance, certified test requirements (CTR's) were drawn up which called upon the contractor to demonstrate, point-by-point, that the specifications were met. For example, the specifications called for an average cabin structural environment of 30° to 130°F. Therefore, a CTR was written which stated that the average value of the thermocouples attached to the cabin pressure shell would be from 30° to 130°F. Moreover, this range was subdivided by mission phase; e.g., 30° to 100°F prior to lunar touchdown, 30° to 130°F during lunar stay, etc. The CTR called out the applicable thermocouple numbers and mission events. Criteria for acceptable simulation of the thermal-vacuum environment were included as part of the CTR's; e.g., a vacuum level of 1×10^{-5} torr or better, and cold walls at

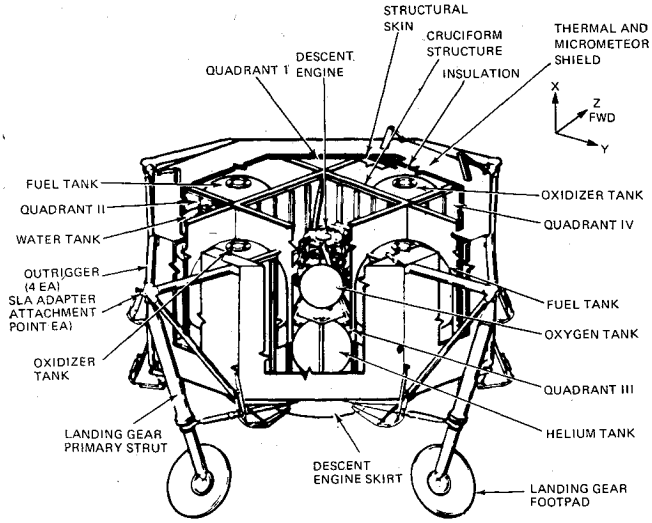

Fig. 2 Descent stage (D/S) general arrangement.

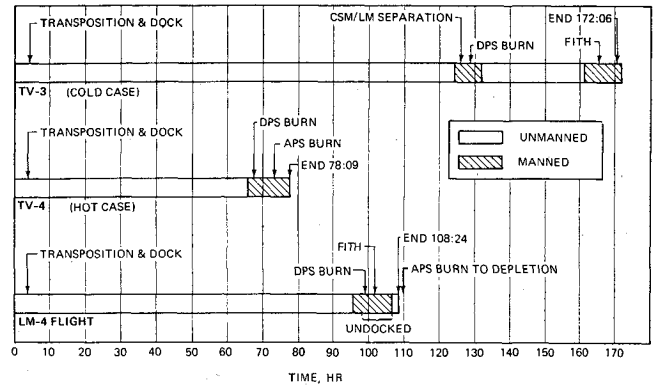

Fig. 3 LM-4 timeline comparison, flight vs test.

−280°F with an emittance of 0.9 or greater. Provisions had to be made to demonstrate that the agreed upon thermal radiation environment was provided. All told 76 CTR's were written to define acceptable performance.

The test plans (OCP's) were usually more detailed than a flight plan. Both the baseline OCP and the multitude of changes required to keep it up to date with current mission thinking were the result of constant cooperative efforts on the part of the contractor and customer. Approximately 3000 pages made up the four test OCP's. A typical timeline comparison between the TV tests and a flight they were to release is presented in Fig. 3.

Test Hardware Description

External Environment Simulation

Heat loads to the vehicle (planetary, direct, and reflected solar radiation) were simulated using electrical energy applied to conformal skin heaters. These heaters were constructed of 0.01-in.-thick aluminum sheets with nickel-copper resistance heater ribbons attached. The ribbons were sandwiched between layers of pressure-sensitive, H-film tape and were attached to cover the surface area uniformly. Individual heaters were constructed so that the external geometric configuration of the LTA-8 duplicated that of flight vehicles. The skins were attached to the vehicle with the heaters facing inboard, and the outboard surfaces were coated to reproduce the emittance of the corresponding area on the flight vehicle. Figure 4 shows the LTA-8 vehicle after final heater skin installation. Selected heaters were wired in series or parallel and connected to specific power modules, controlled by

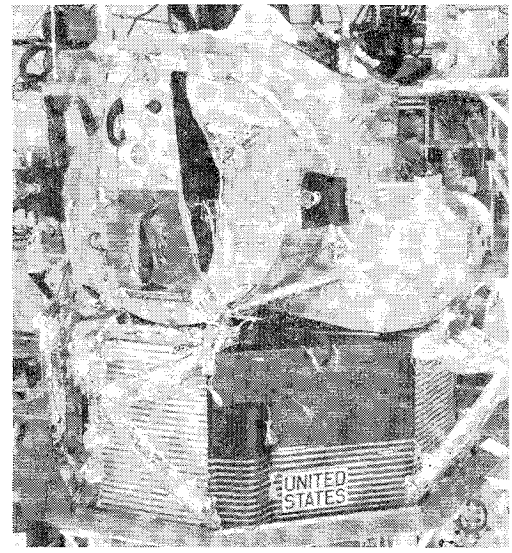

Fig. 4 LTA-8 vehicle.

manually set rheostats. The vehicle was divided into eight major vertical segments which could be ganged together. By selectively supplying power to these segments, translunar roll and planetary heat inputs were simulated in a step fashion. The power supply was capable of controlling each of 480 different heater sets individually through its own module.

The vacuum and sink temperature of space were approximated within Chamber B of the NASA Space Environmental Laboratory at the Manned Spacecraft Center, Houston, Texas. Chamber B is lined with liquid-nitrogen-cooled heat-sink panels that operate at approximately −300°F and are coated to produce measured emittances of greater than 0.90. The vacuum pumping system consists of roughing trains, diffusion pumping and backing trains, and helium panels for cryogenic pumping. It can maintain test pressures near 1×10^{-6} torr. Since the LTA-8 external configuration and emittance matched the flight vehicles, and the chamber emittance approximated that of space, the radiative interchange factors from the individual heaters to each other and to the cold walls duplicated those of flight vehicle surfaces to each other and to space. Therefore, by supplying analytically derived flight heat inputs as electrical energy to the heaters, the external environment of the LTA-8 in the chamber simulated that of the flight vehicles.

Sewer Plate and Command and Service Module Thermal Simulator (CSMTS)

The CSM connects to the LM docking tunnel which is located in the A/S midsection. During docked phases, the connected vehicles transfer thermal energy radiatively from their external surfaces, and radiatively and conductively through the docking tunnel. Neither of these effects is large, representing at most a heat-transfer of 50 Btu/hr. During undocked phases, the docking tunnel views the external environment, and the heat load to the A/S varies from an input of approximately 300 Btu/hr during a full sun phase, to a leak of 175 Btu/hr when the tunnel views space and receives no solar load. Due to chamber size limitations, the CSM had to be replaced with a simulator which could thermally reproduce the docked and undocked phases.

Heat-transfer through the docking tunnel was simulated through the use of a 0.1-in.-thick copper slab ("sewer plate") to which electrical resistance heaters and liquid nitrogen carrying tubes were uniformly attached over the surface. The sewer plate was located on top of the A/S docking tunnel at the exit plane (Fig. 5). Thermocouples were attached to both the sewer plate and tunnel so that during simulated docked phases, an analytically determined temperature difference between the two could be controlled, thereby establishing the desired net heat-transfer rate between the vehicles. During simulated undocked phases, the heaters were turned off, and liquid nitrogen was passed through the cooling tubes to reduce the sewer plate temperature rapidly to −300°F. Heaters were installed within the docking tunnel, so that solar and planetary thermal loads could be introduced.

The external thermal interchange between the LM and CSM was accomplished through the use of the CSM Thermal Simulator (CSMTS). This device consists of a cylinder and "slotted" disk which sits on top of the sewer plate (Fig. 5). It was designed to reproduce the radiative couplings to the LTA-8 that exist between the flight LM and CSM. The surfaces viewing the LTA-8 were coated to match CSM thermal emittances, and were designed so that the area view factor term to the LTA-8 equaled that between the flight vehicles. During docked phases, thermocouples on the CSMTS were used to control attached electrical resistance heaters. To simulate undocked phases these heaters were turned off, and the simulator rapidly approached −250°F. Since the external heat-transfer between the LTA-8 and the CSMTS was small, the fact that the LTA-8 viewed a −250°F CSMTS, rather than a −300°F chamber wall, had little effect on the test results.

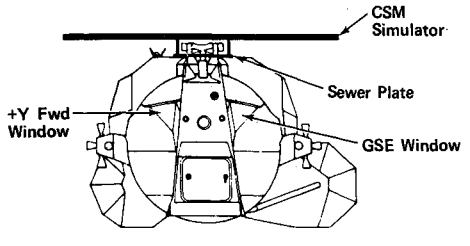

Fig. 5 CSM simulator installation.

Windows

Each window comprises an inner pane, which is a part of the pressure vessel, and an outer pane, which is essentially a micrometeroid shield. Electrical resistance heaters were attached uniformly over the outer panes of the +Y forward and docking windows. The net heat-transfer through the windows was controlled by monitoring the temperature difference between thermocouples mounted to the inner and outer panes. The heat load was analytically predicted through the use of a detailed thermal model which accounted for the energy incident on the outer and inner panes due to direct solar, albedo, and planetary heat inputs, as well as a defog heater input to the inner pane. Computer runs used these analytical heat inputs to determine a temperature difference timeline to be followed during the tests.

The −Y forward window was replaced with an aluminum plate (GSE) containing feed through connectors for electrical power supply and instrumentation cables. An aluminum rod with a heater and a liquid nitrogen "end plate" was attached to the GSE window as shown in Fig. 6. The net heat-transfer was simulated by monitoring two thermocouples, a fixed distance apart (i.e., known thermal resistance), and utilizing the heater and liquid nitrogen flow to the end plate to control the temperature gradient. The net heat-transfer through the −Y forward window was calculated through the use of a detailed thermal model as described earlier.

Ascent and Descent Engine Firings

During a typical burn, heat slowly "soaks" through the engine and is then conducted and radiated to the surrounding structure. This process, which takes considerably longer than the actual engine firing, is called "soakback." An engine burn may last from 10 to 15 min, whereas the associated soakback lasts for 5 to 10 hr. Heaters were installed to simulate engine backface (facing structure) temperatures following a burn. With the exception of the injector, heater wires were attached either directly to prototype engines or to copper plates attached to the engine to conform to the external engine configuration. The external engine parts, copper plate heaters, valves, etc., were coated where necessary to produce flight engine emittances. Figure 7 schematically represents the descent-engine and base heat-shield-soakback heater locations.

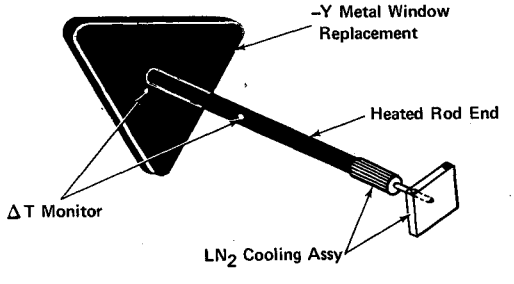

Fig. 6 GSE window simulator.

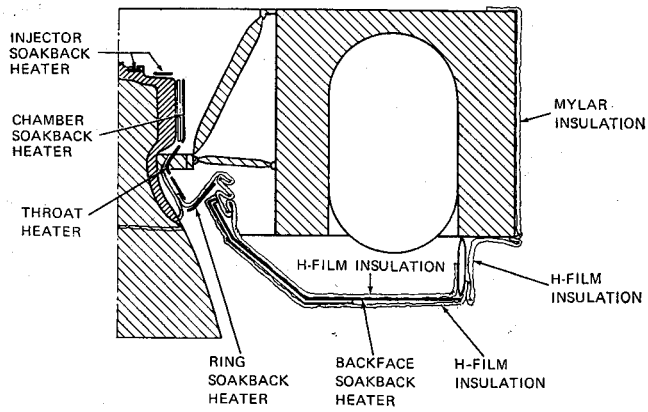

Fig. 7 Descent propulsion system soakback heaters.

This method of simulation adequately duplicates the radiative heat transfer from the engines to each stage but reduces the effect of conduction heat-transfer. It was selected because radiation heat-transfer predominates, being approximately one order of magnitude larger than conduction; e.g., 1 hr after an A/S engine firing, heat-transfer from the engine to the A/S is approximately 2100 Btu/hr by radiation, as compared to 250 Btu/hr by conduction. The temperature profiles of the engine backface surfaces were determined from detailed analytical models of the engines and their structural interfaces. Real time tracking of the heater temperatures during the test insured adequate reproduction of the soakback temperature profiles. Figure 8 presents typical comparisons of the desired (flight) response to the driven (test) response for engine heaters. The engine backface heaters were driven to temperature as high as 700°F.

During D/S engine firings, the engine skirt is heated by the exhaust gas and in turn radiates to the D/S base heat shield. The heat subsequently soaked through the backface titanium and H-film insulation into the structure (Fig. 7). To simulate this heat soakback, woven wire mesh heaters were mounted to the titanium support structure. Again, soakback was reproduced by driving the titanium backface temperature profiles to an analytically determined response. Base-heat-shield temperatures as high as 950°F were simulated.

RCS Engine Firings

The soakback effect from RCS engine firings is less significant to the A/S than an ascent engine burn. However, to simulate it, heaters were installed in the injectors and were driven to predicted profiles following simulated firings. Typically the injector temperature response was driven from 15 to 30 min, raising the heater temperature to as high as 300°F.

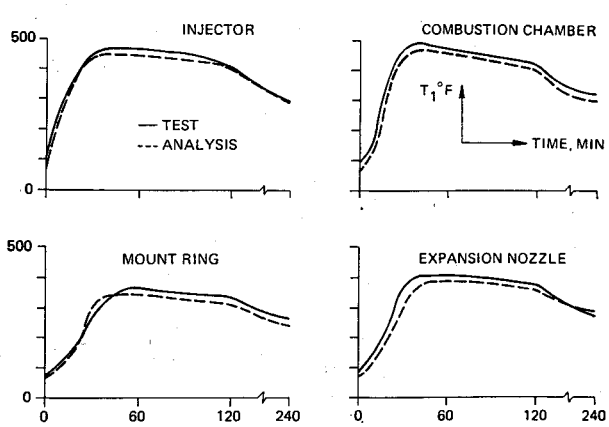

Fig. 8 Ascent propulsion system soakback profiles.

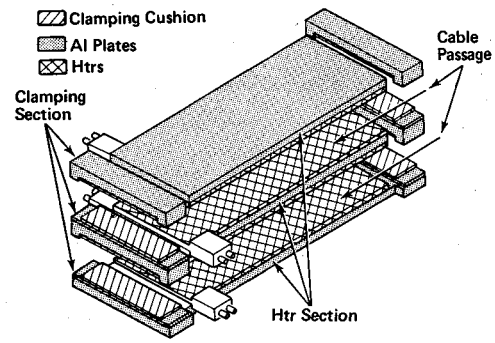

Fig. 9 Cable guard heater.

Guard Heaters and Vehicle Instrumentation

The LTA-8 required numerous ground-support connections to implement the test program. These included power-supply cables, propulsion-tank fill and drain lines to aid in engine firing simulations, instrumentation cables, cabin gas lines, etc. These penetrations introduced heat leaks not found in the flight vehicles. To eliminate the conduction heat transfer from the LTA-8 interior through the lines, the latter were routed through guard heaters. A fluid line guard consisted of a short section of metal tubing, heated by a sheathed resistance wire, wound around, and brazed to the tube. When in use, the tube replaced a section of the fluid line just outboard of the vehicle skin. The electrical line guard heaters were all similar to that shown in Fig. 9. The heater section was basically a stack of electrically heated plates, with the cables sandwiched between them. This assembly was mechanically clamped together. Temperature control was accomplished with an automatic system which compared the guard temperature with the vehicle interface temperature, and cycled power to the heaters whenever the difference exceeded 1°F. The length of lines between the guards and the vehicle interface were wrapped with multilayer insulation.

The test data had to satisfy two requirements: 1) provide sufficient information for a complete post-test analysis, including a network verification and flight capability, and 2) provide nearly real-time information to the engineering support personnel to advise the test team of any required changes in the test flow. Nearly 2000 measurements were utilized to monitor the vehicles structure, vehicle subsystems operation, heater inputs, test chamber conditions, and astronaut physiological conditions. A summary of the instrumentation pertinent to thermal testing is presented in Table 1 (Ref. 4).

External Skin Inputs

By programing the individual heater skins as required, any vehicle orientation timeline can be simulated and there is no need for internal chamber hardware, such as turntables or gimbal arms. Since the environmental radiation load is not absorbed by the skin, the external vehicle coating does not require the prototype thermal absorptance. However, it is necessary to duplicate flight emittances to assure proper couplings between skins and from skins to space. Another benefit is that the electrical power input is stable, uniform, and can be accurately measured and controlled, so that the analyst knows at all times what the thermal load is. Limited simulation of different vehicle coatings can be done by applying an appropriate scaling factor to the power levels. Finally, the loss of an individual heater during a test affects only a small area, and can be rectified by increasing the power level to adjacent skins to compensate for the local loss.

While there is no uncertainty as to the magnitude of the actual test inputs, the desired value is the result of a theo-

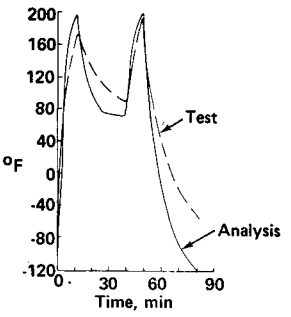

Fig. 10 Typical skin response.

retical analysis. To perform this analysis, the external vehicle is divided into isothermal surfaces or nodes. The nodes selected, represent areas which absorb and emit energy uniformly over their surfaces. Planetary and solar heat loads were calculated with the aid of the following programs.

1) Diffuse solar program determines the net amount of direct solar energy absorbed by a vehicle with diffusely reflecting surfaces. A maximum of 200 planar surfaces may be considered, including intervening surfaces.

2) Orbital heat flux program determines albedo and IR heat fluxes from a given planet to an orbiting vehicle. Intervening surfaces are not taken into consideration and must be evaluated.

3) Lunar surface calculation program to evaluate the IR and albedo input, the lunar surface visible to the vehicle is divided into finite areas, and the couplings between the skins and the surface is determined. Using these couplings, the lunar surface temperature and the albedo, the emitted and reflected energy input to the skins is obtained.

The described heat inputs are combined to form the power level corresponding to the desired vehicle orientation. For example, when the vehicle is in Earth orbit, the heat load to the skins results from the addition of direct solar and orbital heat inputs. Similarly, translunar, lunar orbit, and lunar surface loads are constructed from one or more of the above determined heat loads. Simple geometric relationships existed between the analytical nodes and power controllers, and were used to form nodal to power controller conversions. Using these conversions, the test heat inputs were calculated for the various mission phases.

Test Results

Heater Difficulties

The validity of the technique may be evaluated by comparing the predicted skin temperature profile to the actual test results. Comparisons made after the TV-1/TV-2 tests indicated a number of anomalies. In certain areas individual skin temperatures ran considerably above predicted values. A review of the test configuration led to the conclusion that these skins did not have the anticipated view to the cold walls. Various GSE hardware physically blocked the skins, thus causing an unexpectedly higher environmental temperature. Throughout the remainder of the program this continued to be a problem. It was overcome for most cases by using the test data to evaluate the degree of blockage, and then adjusting the desired input accordingly. In keeping with the worst case test philosophy, these (downward) adjustments were made for all cold case tests, and in the hot case only where safe skin temperatures were exceeded. For the more typical case where no problems were encountered, test and predicted data show acceptable agreement. Figure 10 illustrates this comparison for a typical skin. The average radiating temperature of the test and analytical profiles presented agree to within ±1°F.

Table 1 Vehicle instrumentation

Description	Flight operational[a]	Development flight[b]	Test
Temperature	35	94	1131
Pressure	14	5	18
Flow rate	...	...	2
Voltage	47	8	55
Current	11	...	285

[a] LM-4 and subsequent vehicles contain only operational instrumentation.

[b] LM-3 vehicle contained development as well as operational instrumentation.

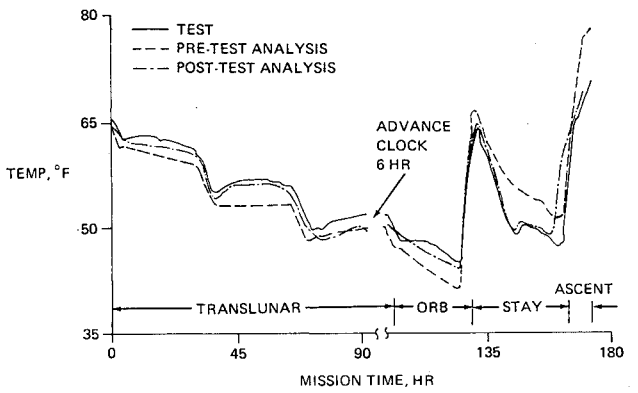

Fig. 11 LTA-8 typical test results.

Network Verification

Since a perpetual series of test and flight cycles is not desirable, the testing constraint had to be eliminated eventually. To this end, verification of the analytical thermal networks was performed, so that they could be used with a high degree of confidence to predict flight thermal response. The determination of the temperature distribution within a vehicle involves the solution of the transient heat-transfer equation with prescribed boundary and initial conditions. The thermal analyzer technique requires that the heat-transfer problem be represented by an analogous nodal network connected by thermal connectors and radiators. Using engineering judgment, the vehicle is divided into isothermal areas, each represented by a nodal center. In addition to the main vehicle thermal balance for the A/S and D/S, networks representing the ECS active coolant loop and the crew compartment were incorporated into the A/S analog. The networks contain approximately 700 nodes and 4000 conductors (conduction, radiation, and convection).

The Grumman Thermal Analyzer computer program (GTA-1) writen for the IBM 360/75, solves a heat balance equation at each node. It can be used to obtain temperature distributions and heat fluxes for transient or steady-state conditions on any three-dimensional configuration. Problems may involve heat generation and heat transfer by conduction, convection, and radiation. Physical properties may vary with temperature or time. Subroutines evaluating heat-transfer rates, ECS loop response, etc., have been written and are used extensively. For mission analysis purposes, external heat inputs, equipment heat dissipation, ECS parameters, etc., are fed into the program and activated to conform to flight timelines. Engine firings effects are analyzed by driving critical engine backface temperature profiles following a burn. These burn profiles are obtained from detailed analyses and testing of the engines and their surrounding structure.

For the LTA-8 test program, pretest analyses were run using the planned test timelines to insure that the test objectives were realistic and to indicate any potential test problems. The analyses were extremely valuable to the support team for real time test evaluations.

During the test, the operational timelines were altered as circumstances dictated. Events were time shifted, cancelled

Table 2 Flight to test data comparison

Hardware description	Data range, °F[a] LTA-8 TV-3/4	Apollo 10/LM-4	Apollo 11/LM-5	Apollo 12/LM-6
A/S average cabin	45–95	50–70	58–75	59–69
Aft bulkhead	42–82	60–70	64–68	61–73
Propulsion tanks	48–81	69–71	61–72	60–70
RCS tanks	45–87	51–74	68–73	65–73
Low temp electronics Glycol[b]	35–50	37–48	37–48	36–48
D/S propulsion tanks	51–85	67–71	51–74	60–70

[a] Over-all mission phases.
[b] ECS loop flow temperature.

or added to enable test personnel to perform critical test operations in a timely manner. Many of these constraints were caused by the time limitation on the crew's activities during hard-vacuum conditions. Therefore, to accurately evaluate the network response, it was necessary to perform a post-test analysis using as-run timelines. In addition, the post-test analyses utilized the test driven engine burn profiles and critical boundary temperatures, eliminating the need for the evaluation of differences between conditions analyzed and tested. References 5 and 6 detail the results of the network verification performed following the LM-3 (Apollo 9) and LM-5 (Apollo 11) test series. Figure 11 presents a comparison of the LM-5 test and pre- and post-test results for the A/S "average cabin." The average cabin is a significant thermal parameter used to indicate the average crew environment temperature. The results presented are typical and show that the post-test analysis tracks the test response closer than the pretest. Additionally, the results verified the ability of the analytical model to predict average cabin response. The network verification effort uncovered several model difficiencies. However, sufficient thermal test data was obtained during the tests to modify the model and improve its ability to predict test results. In general, the modifications included: conduction updates, radiation updates, addition of nodes, etc.

Comparison of Flight to Test Data

A comparison of test to flight data temperature ranges is presented in Table 2. To date, three lunar missions have been flown and as shown, the recorded flight data has been within anticipated ranges. In every case, the flight data is within the band of test results. This shows that, as intended, the test vehicle was exercised over a more severe mission than actually flown. Detailed comparisons of flight results to preflight analyses show excellent agreement.

Conclusion

The LTA-8 series showed that manned worst-case mission simulation testing in the thermal-vacuum environment is feasible. For the LM program, it provided the final thermal certification of vehicle systems and analytical techniques required for release of the flight mission. In a similar fashion, the data obtained from completed Apollo missions has attested to the thoroughness of the simulations and the validity of the results, thus providing increased confidence in the success of more complex missions. Two thermal vacuum testing "innovations" were the use of conformal skin heaters to simulate the thermal environment of manned spacecraft, and the real time vacuum entry and egress of test subjects into the spacecraft.

References

[1] Bartilucci, A., Lee, E., and Tawil, M. N., "LM Passive Thermal Design and Test," AIAA Paper 68-748, Los Angeles, Calif., 1968.

[2] Tawil, M. N. and Caloger, P., "The Use of Multilayer Insulation on the LM Vehicle," AIAA Paper 69-609, San Francisco, Calif., 1969.

[3] "Contract Technical Specification for Lunar Module System," LSP-470-1D, Nov. 1968, Grumman Aerospace Corp., Bethpage, N. Y.

[4] Hellman, R. et al., "Lunar Module Thermal Vacuum Simulation Utilizing Conformal Heater Thermal Control," AIAA, Paper 69-312, Houston, Texas, 1969.

[5] "90 Day Thermodynamics Report, LTA-8/D Mission Simulation," LTR-510-4, Oct. 1968, Grumman Aerospace Corp., Bethpage, N. Y.

[6] "90 Day Thermodynamics Report, LTA-8/G Mission Simulation," LTR-510-6, May 1969, Grumman Aerospace Corp., Bethpage, N. Y.